INDIAN JOURNAL OF SCIENCE AND TECHNOLOGY

RESEARCH ARTICLE

# Determination of sky status by ground based radiometric data analysis

**Manabendra Maiti[1], Kausik Bhattacharyya[2], Salil Kumar Biswas[3], Md Anoarul Islam[1], Ayan Pradhan[4], Judhajit Sanyal[1]***

**1** Department of Electronics & Communication Engineering, Techno International New Town, Kolkata, 700156, West Bengal, India
**2** Department of Physics, Tamralipta Mahavidyalaya, Tamluk, East Medinipur, 721636, West Bengal, India
**3** Department of Physics, University of Calcutta, 92 A.P.C Road Kolkata, 700009, West Bengal, India
**4** Department of Electronics, Acharya Prafulla Chandra College, New Barrackpore, Kolkata, 700131, West Bengal, India

OPEN ACCESS

**Received:** 17.03.2021
**Accepted:** 19.07.2021
**Published:** 04.08.2021

**Citation:** Maiti M, Bhattacharyya K, Biswas SK, Islam MA, Pradhan A, Sanyal J (2021) Determination of sky status by ground based radiometric data analysis. Indian Journal of Science and Technology 14(27): 2250-2256. https://doi.org/10.17485/IJST/v14i27.447

* **Corresponding author**.

judhajit.sanyal.2019@gmail.com

**Funding:** None

**Competing Interests:** None



Published By Indian Society for Education and Environment (iSee)

**ISSN**
Print: 0974-6846
Electronic: 0974-5645

## Abstract

**Objectives:** To predict meteorological phenomena such as rain events from sky status during rainy and non-rainy periods. **Methods:** The method used here is based on brightness temperature ratio measurement at two different frequencies, namely 23.8 GHz and 30 GHz respectively, using ground based dual frequency radiometric data. The ratios of brightness temperature readings obtained by the dual-frequency radiometer at the two above mentioned frequencies are calculated for each simultaneously-taken pair of measurements. Data obtained by the authors for the year 2009 at Cachoeira Paulista in Brazil has been used for analysis. **Findings:** The major results obtained from the analysis of data collected over a continuous period of seven months are used to construct corresponding histograms and cumulative count graphs of brightness temperature ratios. The histograms and graphs clearly show three peak values that could be interpreted as thresholds between clear sky, cloudy sky and rainy sky conditions respectively. **Novelty:** The study implements detection of rain events from sky status during rainy and non-rainy periods using peak brightness temperature values obtained from graphs generated using the observation data. The outlined technique can therefore be used to clearly determine sky conditions and accurately predict rain phenomena. The ratio of brightness temperatures at the two frequencies is a unique parameter which is critical to the successful estimation of rain from sky status. The results agree well with multi-channel radiometric data obtained by other researchers at lower frequencies.

**Keywords:** sky status; microwave; millimeter wave; dual frequency radiometer; brightness temperature; rainfall

## 1 Introduction

To meet the growing needs of higher data rates for present day communications and multimedia systems, use of electromagnetic spectrum above 10 GHz in microwave and millimeter wave region is an obvious solution. However the signals in this frequency range get impaired by rain that causes serious attenuation especially in tropical and equatorial countries that are characterized by heavy rainfall. A ground based microwave radiometer[1,2] has proved its utility to monitor the atmosphere up to 10 Km continuously by measuring very low level microwave radiation at some specific frequency channels in the microwave bands dominated by atmospheric water vapor, cloud liquid water and molecular oxygen emissions. Geophysical observables such as the total amount of water vapor (PWV), the non-precipitating cloud liquid content (LWC) and rain are have frequently been used to develop models[3,4].

Applications of the ground-based microwave radiometer to measure meteorological parameters have been widely accepted for years[5]. Long-term analysis of sky thermal emissions (Tb's), from single ground-based microwave radiometers during massive measurement campaign or from radiometric-networks, could benefit from some analytic criterion to detect data affected by rain events. Brightness temperatures ($T_b$'s) measured at the ground level, within the frequency range of 20-30 GHz under rainy conditions are not appropriate to retrieve the above mentioned quantities[6].

Ulaby suggested that the brightness temperature given by ground based microwave radiometer obeyed the radiative transfer equation under scatter-free conditions[7]. The determination of rainfall signature requires some thorough insight into the electromagnetic interaction between microwave radiation and the medium concerned, since radiometric response depends on various radiative sources and the atmospheric inhomogeneity posed by hydrometeors in different phases.

The identification of rainy periods is of importance also for the telecommunication systems operating at Ka and Q/V bands, where a major impairment derives from the effect of the lowest layers of the atmosphere on radio-wave propagation[8].

High values of power margin can be reduced if a priori information of atmospheric conditions along a propagation path is known to us and favours the adoption of adaptive fade mitigation technique[9].

The idea of short term rain prediction by considering the pronounced increase of brightness temperature from two hours before a rain event in the water vapour channel[10] gave impetus to the authors' thoughts on finding an identifying demarcation between no rain and rain events. Bosisio and Capsoni[11] devised a relation between the two brightness temperatures at the frequencies 23 GHz and 31 GHz based on the radiative transfer forward model[12], through analysis of month-long experimental data as a part of the Dutch CESAR project. Due to the response of microwave radiometric channels (at 20-30 GHz), which have a different sensitivity to the atmospheric constituents, a possible way to detect rainy radiometric data could be based on the ratios between pairs of $T_b$'s.

The ratio between $T_b$'s appears more suitable as an indicator than the single channel brightness temperature itself to discriminate sky conditions. In fact, a linear relationship between $T_b$'s jointly measured around 20 and 30 GHz exists under clear sky conditions, while it becomes strongly non-linear in the presence of heavy clouds or rain events[13]. Also, it is observed that specific temperature ratio values can be related to different atmospheric scenarios, ranging from clear to rainy sky[11].

In recent years, a number of novel approaches to the problem have been proposed by authors. Machine learning-based methods have been implemented in[14], while optical imaging has been employed with a suitable degree of success in[15]. The work presented in[15] is of specific interest as it does not employ radiometers; however the drawback of the work lies in the limitations of accurate optical imaging for a number of different atmospheric conditions, especially for tropical regions. A similar work presented in[16] is effective provided there are no obstructions, and the variation in meteorological parameters is prominent and hence detectable by optical means with an acceptable degree of accuracy. The drawbacks of purely optical imaging can be addressed through a hybrid system which allows for radiometric sensing as well as optical imaging, used in deep space exploration[17]. Pyranometric measurement techniques have also been explored as a viable solution in[18]. However recent models employing brightness temperature measurements for meteorological estimation have been found to yield accurate results for the 0.5-2 GHz band[19].

The authors of this paper have used the relationship between $T_b$'s to gather information to discriminate between clear and rainy atmospheric conditions from the output of a radiometer placed at the tropical location of Cachoeira Paulista (22.57 deg. S, 89 deg. W), INPE, Brazil. The ratio between $T_b$'s is seen as the critical factor which can be used to differentiate between different sky conditions and consequently evaluate the occurrence of meteorological phenomena such as rain.

## 2 Methodology

Under clear sky, the brightness temperature $T_b$ (K) at a radiometric frequency $f_i$ is given by Bosisio[3,8].

$$T_b(f_i) = a_i V + b_i \tag{1}$$

Here $a_i$ ($Kmm^{-1}$) and $b_i$ (K) are frequency and elevation angle dependent coefficients. The Precipitable water vapour (PWV) is expressed by the term V ($mm^{-1}$).

These coefficients are evaluated by linear curve fitting for a large radio sounding database and concurrent radiative transfer forward modelling by Bosisio and Mallet[12]. Under clear weather only considering the water vapour contribution to the brightness temperature the above relation was put forwarded as a part of dual frequency algorithm.

In the present work, data for one year (2009) was obtained from Cachoeira Paulista in Brazil, where the variations in meteorological phenomena showed variance equivalent to the observations expected at tropical locations in Asian countries such as India. Thus the specific location allowed for more extensive modelling as well as helped to augment the statistical validity of the results obtained through application of the model. The data obtained was not modified in any manner to ensure generalizability of the results obtained, especially considering the fact that a slight change in the data might result in the loss of significant information. The observed brightness temperatures at the two frequency channels 23.834 GHz and 30 GHz are taken as $T_b(23.8)$ and $T_b(30)$ respectively and are related in the following equation 2,

$$T_b(30) = c_0 T_b(23.8) + c_1 \tag{2}$$

Here, $c_0 = T_b(30)/T_b(23.8)$, $c_1 = T_b(30) - c_0\, T_b(23.8)$

The choice of frequency 23.834 GHz lies in the fact that it is far away from the pressure broadened water vapour resonance line at 22.234 GHz; hence its independent nature with respect to pressure broadening can help in elimination of any unwanted signal. The other one i.e. 30 GHz lies in weak water vapour attenuation region. It has also been found that the choice of this frequency pair is optimal[4,20] for the measurement of vapour and liquid water.

So long as the sky remains clear the relation between the brightness temperatures at the chosen frequencies stands linear. The building of cloud and rain events however causes a change in the nature of the relationship[13]. With the passage of time, as the liquid phase fills the atmosphere, the clear weather atmospheric path characteristics hidden in the ratio $T_b(30)/T_b(23.8)$ are no longer able to describe the phenomenon of signal variation, rather an idea of unbiased brightness temperature $T_b'(30)$ can be used in this situation.

$$\text{Unbiased } T_b'(30) = T_b(30) - c_1 \tag{3}$$

Considering a change in the linear relationship between $T_b(23.8)$ and $T_b(30)$ when sky conditions change from clear to cloudy, a ratio $T_b(R)$ is proposed to discriminate between clear, cloudy and rainy weather.

$$T_b \text{ Ratio } = T_b'(30)/T_b(23.8) \tag{4}$$

## 3 Results

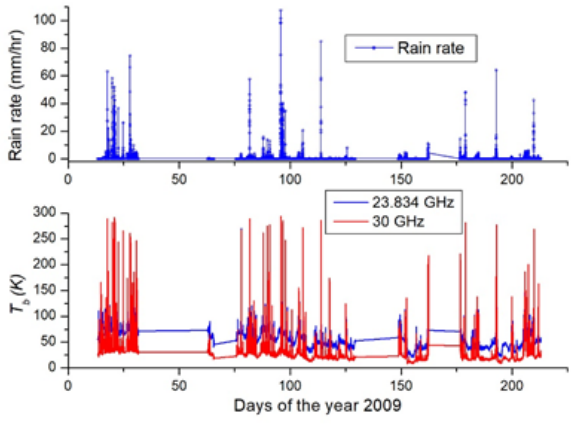


**Fig 1.** (a) Co-located rain gauge data (b) measured brightness temperature at 23.834 and 30 GHz

The time series presentation of brightness temperatures at the two frequencies 23.834 GHz and 30 GHz is shown in Figure 1. The co-located rain gauge data is also shown in the same figure. It is to be mentioned here that the radiometer is recording data throughout the year at a tropical location Cachoeira Paulista (22.57 deg. S, 89 deg. W), INPE. Here it is to be noticed that the few minutes before raining the brightness temperatures underwent a marked increase.

The linear relation between the two brightness temperatures for the said frequencies are studied by plotting the brightness temperatures(K) at two frequencies for a period of more than 225 days along with the entire event of rainy and non rainy period of same length of time and is presented in Figure 2. During clear weather the brightness temperatures shows a linear relation where the coefficients $c_0$=0.41 (dimensionless ratio) and $c_1$=4.944(K). The interaction of rain in liquid phase with the signal along the radio path brings about a change in the values of brightness temperatures (K), which is observable during a spell of rain. If the rain spell is of low intensity, the rise of brightness temperatures (K) is not as high as the rise observed corresponding to a spell of intense rain. Hence, the presence of more rain in liquid phase is reflected in the strong interaction of the rain with the signal.

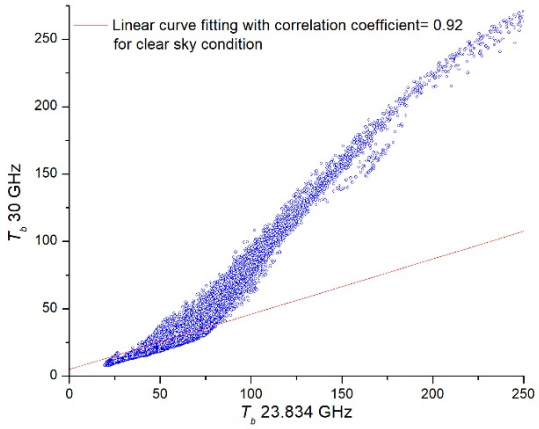


**Fig 2.** Scatter plot of measured $T_b$ at 23.834 and 30 GHz along with linear correlation

The ratio between the temperatures as described in equation 4 along with its time derivative for the time series of the brightness temperatures (K) for the same length of time span are depicted in the Figure 3. As per the discussions in the above paragraph as more and more rain liquid throngs the radio path, brightness temperature rises to a greater extent showing the greater interaction of the signal with the rain liquid; correspondingly the ratio changes, exhibiting its sensitivity to the change in brightness temperature.

A statistical analysis of the number of rain events over Cachoeira Paulista (CP, 220 S), Brazil during the year 2009 reveals that the total number of rain events observed is above 50 (shown in Figure 4 (a)). Out of the total number of observations obtained for these events cumulatively, the number of occurrences goes beyond 200 for rain rates up to 15 mm/hr but quite interestingly it is observed also that the number of occurrences suddenly falls to 70 considering rain rates between 15-25 mm/hr. This suggests that at the place of experiment, the most abundant rain rate was up to 25 mm/hr as shown in Figure 4(b).

Scatter plot of the ratio R and the brightness temperature (K) for rainy events {light rain, medium/heavy rain and all rainy events} are presented in Figure 5. The $T_b$Ratio can explain all these curves by mentioning a threshold of rainy situation value to establish a transitional point to indicate the status of the sky.

The regression analysis of light rain ($T_{b30}$<65) shows the linear relationship corresponding to the regression relation shown below in equation 5.

$$T_b \text{ Ratio } = 0.17724 + 0.00836 T_{b30} \tag{5}$$

The correlation coefficient corresponding to the regression relationship depicted in equation 5 is 0.894. Similarly, for medium and heavy rain ($T_{b30}$>65) the regression relationship has a non-linear nature, which is shown in the following equation 6.

$$T_b \text{ Ratio } = 0.34265 + 0.00688 T_{b30} - 1.60598\text{E}-5 T_{b30^2} \tag{6}$$

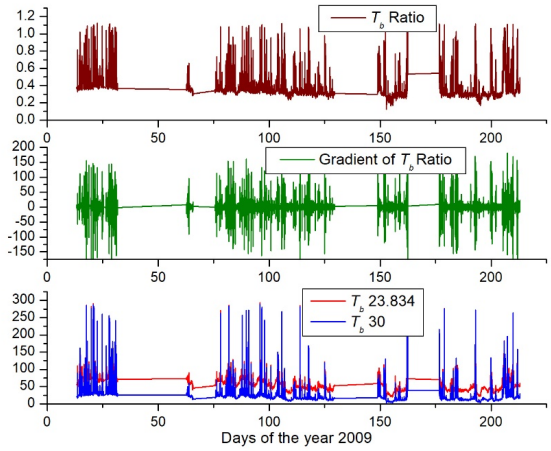


**Fig 3.** Discrimination capabilities of $T_b$ Ratio: from top to bottom, $T_b$ ratio time series, $T_b$ ratio time derivative, $T_b$23.834 and $T_b$30 time series.

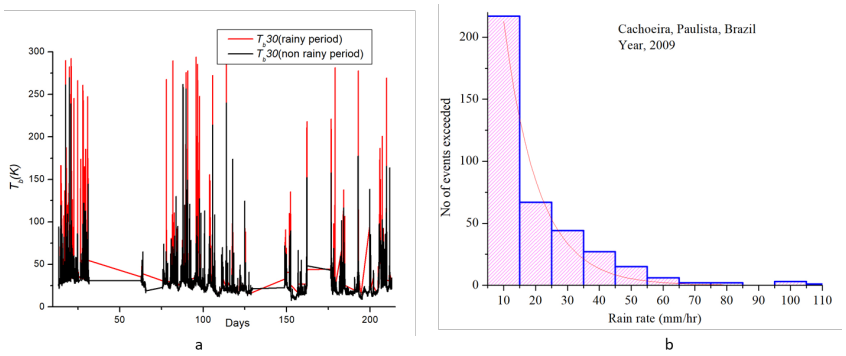


**Fig 4.** (a) Time series of measured brightness temperature at 30 GHz for non rainy (black line) and rainy (red line) periods, (b)-Histogram of rain rate (mm/hr) over Brazil, in the year 2009.

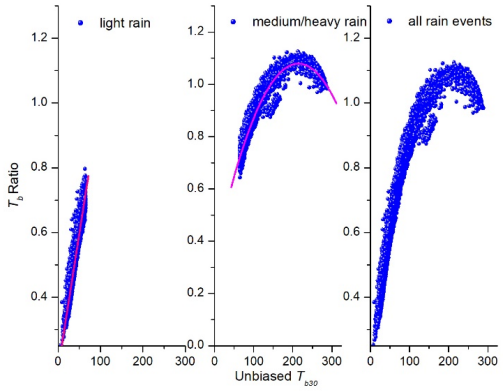


**Fig 5.** Scatter plots between $T_b$Ratio and unbiased $T_{b30}$ during rainy events: (from left to right) light rain event; medium/heavy rain event; all rainy events.

The correlation coefficient corresponding to the above equation is 0.923.

The plot of the histogram of $T_b$Ratio in the following Figure 6c shows 3 peak values that could be interpreted as thresholds between clear sky, cloudy sky and rainy sky, respectively (see Table 1). These three different regions are also visible in the histogram of $T_b$30 values shown in Figure 6d. The Cumulative Distribution Function (CDF) plots reveal these thresholds in term of different slope regions seen in Figure 6a and Figure 6b respectively.

**Table 1.** Sky conditions:$T_b$ Ratio and $T_b$ 30 threshold values

| | $T_b$Ratio | $T_b$ 30(K) |
|---|---|---|
| Clear sky | 0.321-0.459 | 13.75-29.75 |
| Cloudy sky | 0.459-0.768 | 29.75-65.25 |
| Rainy sky | >0.768 | >65.25 |

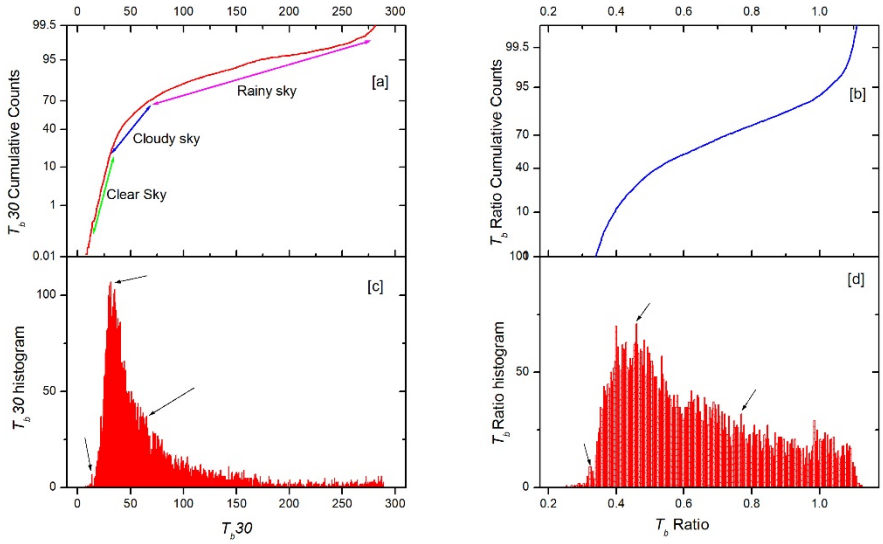


**Fig 6.** Statistical characteristics (a): CDF of$T_b$ 30 (b): CDF of $T_b$ Ratio (c): Histogram of $T_b$ 30 (d): Histogram of $T_b$ Ratio.

## 4 Discussions

The ratio of radiometric brightness temperatures at two different frequencies seems to be a good tool for identifying the sky status. In this paper brightness temperature data corresponding to 23.8 and 30 GHz is used to determine sky conditions by differentiation of clear, cloudy and rainy sky $T_b$ Ratio value ranges of 0.321-0.459, 0.459-0.768 and greater than 0.768 respectively. Considering the analyzed data, sky status indicator has been associated at clear, cloudy and rainy sky conditions assuming values up to 0.39, between 0.4 to 0.88 and greater than 0.88, respectively. A validation of the said parameter classification capability has been performed using concurrent brightness temperatures at 15 GHz, collected by an independent radiometric unit with the ability to sense emission processes. The validation, although limited, has indicated that the proposed indicator has a very good potential for correctly assessing sky conditions to adjust communication systems accordingly. A significant level of similarity was found in the findings presented in this work and the results obtained in [19] at much lower frequencies for ice measurements. However, the use of brightness temperature in the present work is novel and allows for comparatively greater accuracy of the corresponding statistical model, since the dual frequency measurements allow for smoothing of the CDF. This leads to more meaningful statistical results. Also, since a simple quadratic curve-fitting methodology is outlined in the work, the corresponding algorithm is expected to run in linear time, that is, with an O(n) time complexity.

## 5 Conclusion

Sky status is important for designing fade margins for satellite communication systems. Advantages in the use of the sky status indicator for optimal functioning of satellite communication systems are in the easy software implementation of the measurement and sky status determination algorithm and in the online system performance monitoring capability so that dynamic fade mitigation techniques could be designed and systems set up, to contrast possible degradation of a satellite propagation channel due to scattering processes arising from rain. The determination of the brightness temperature ratio as a critical factor in the estimation process is a major contribution of the present work. This allows for greater statistical accuracy of the proposed model with fairly linear time complexity for quadratic model establishment, which can allow distributed simultaneous estimation to be implemented using IoT based devices, in future. The accurate estimation of sky status is therefore made possible. As a consequence, through application of the technique illustrated in this paper, rain events can be accurately predicted from sky status, which in turn can allow communication systems to adjust signal parameters accordingly to mitigate rain related effects. In the future, the authors intend to implement the technique outlined in the work on a distributed platform, with the estimation technique enhanced by the application of low time-complexity machine learning algorithms, which are expected to significantly increase the efficacy of the proposed technique.

## References


1) Czekala H, Crewell MS, Simmer C, Thiele A, Hornbostel A, Schroth A. Interpretation of polarization features in ground-based microwave observations as caused by horizontally aligned oblate spheroids. *Journal of Applied Meteorology*. 2001;40:1918–1932.
2) Liua GR, Liub CC, Kuoc TH. Rainfall intensity estimation by ground-based dual-frequency microwave radiometers. *Journal of Applied Meteorology and Climatology*. 1035;40(6):1035–1041. Available from: https://doi.org/10.1175/1520-0450(2001)040<1035:RIEBGB>2.0.CO;2.
3) Bosisio AV, Fionda E, Ciotti P, Martellucci A. Rainy events detection by means of observed brightness temperature ratio. In: 12th Specialist Meeting on Microwave Radiometry and Remote Sensing of the Environment (MicroRad). 2012;p. 1–4. doi:10.1109/MicroRad.2012.6185244.
4) Karmakar PK, Maiti M, Sett S, Angelis CF, Machado LAT. Radiometric estimation of water vapor content over Brazil. *Advances in Space Research*. 2011;48(9):1506–1514. Available from: https://dx.doi.org/10.1016/j.asr.2011.06.032.
5) Janssen M. Atmospheric remote sensing by microwave radiometry. New York, 572. John Wiley. 1993.
6) Marzano FS, Cimini D, Ciotti P, Ware R. Modeling and measurement of rainfall by ground-based multispectral microwave radiometry. *IEEE Transactions on Geoscience and Remote Sensing*. 2005;43(5):1000–1011. Available from: https://dx.doi.org/10.1109/tgrs.2004.839595.
7) Ulaby FT, Moore RK, Fung AK. Microwave Remote Sensing-Active and Passive;vol. 1. Norwood. Artech House. 1986.
8) Bosisio AV, Fionda E, Basili P, Carlesimo G, Martellucci A. Identification of rainy periods from ground based microwave radiometry. *European Journal of Remote Sensing*. 2012;45(1):41–50. Available from: https://dx.doi.org/10.5721/eujrs20124505.
9) Shih S, Chu Y. Studies of 19.5 GHz sky radiometric temperature: Measurements and applications. *Radio Science*. 2002;37:1–16. Available from: 10.1029/2000RS002596.
10) Hye YW, Yeon-Hee K, Hee-Sang L. An application of brightness temperature received from a ground-based microwave radiometer to estimation of precipitation occurrences and rainfall intensity. *Asia-Pacific Journal of Atmospheric Sciences*. 2009;45(1):55–69.
11) Bosisio AV, Capsoni C. Effectiveness of brightness temperature ratios as indicators of atmospheric path conditions, Microwave Radiometry and Remote Sensing of Environment. *VSP*. 1995;p. 129–138.
12) Bosisio AV, Mallet C. A three frequency non linear algorithm for water vapor and liquid water content retrieval. In: Progress in Electromagnetics Research Symposium-ESTEC Centre;vol. 94. 1994;p. 11–15.
13) Mallet C, Lavergnat J. Beacon calibration with a multifrequency radiometer. *Radio Science*. 1992;27(5):661–680. Available from: https://dx.doi.org/10.1029/92rs00817.
14) Bhattacharyya K, Maiti M, Biswas SK, Islam MA, Pradhan AK, Ghosh PK, et al. Short Term Rain Forecasting from Radiometric Brightness Temperature Data. *Journal of Mechanics of Continua and Mathematical Sciences*. 2020;15(2):70–83. Available from: https://doi.org/10.26782/jmcms.2020.02.00007.
15) Alonso-Montesinos J. Real-Time Automatic Cloud Detection Using a Low-Cost Sky Camera. *Remote Sensing*. 2020;12:1382–1382. Available from: https://dx.doi.org/10.3390/rs12091382.
16) Liandrat O, Cros S, Braun A, Saint-Antonin L, Decroix J, Schmutz N. Cloud cover forecast from a ground-based all sky infrared thermal camera. 2017. doi:10.1117/12.2278636.
17) Ely TA, Seubert J, Bradley N, Drain T, Bhaskaran S. Radiometric Autonomous Navigation Fused with Optical for Deep Space Exploration. *The Journal of the Astronautical Sciences*. 2021;68(1):300–325. Available from: https://dx.doi.org/10.1007/s40295-020-00244-x.
18) Alani OE, Ghennioui H, Ghennioui A, ezzahra Dahr F. Detection of clear sky instants from high frequencies pyranometric measurements of global horizontal irradiance. In: E3S Web of Conferences 229;vol. 229. 2021. Available from: https://doi.org/10.1051/e3sconf/202122901008.
19) Jezek KC, Johnson JT, Tan S, Tsang L, Andrews MJ, Brogioni M, et al. 500-2000-MHz Brightness Temperature Spectra of the Northwestern Greenland Ice Sheet. *IEEE Transactions on Geoscience and Remote Sensing*. 2018;56(3):1485–1496. Available from: 10.1109/TGRS.2017.2764381.
20) Karmakar PK, Maiti M, Calheiros AJP, Angelis CF, Machado LAT, Costa SSD. Ground-based single-frequency microwave radiometric measurement of water vapour. *International Journal of Remote Sensing*. 2011;32(23):8629–8639. Available from: https://dx.doi.org/10.1080/01431161.2010.543185.